




RESEARCH ARTICLE | MARCH 13 2023

Effect of surface radiation on the surface heat flux of two-dimensional hypersonic panel flow

Bingfei Yan (严炳蜚) ; Guannan Zheng (郑冠男)  



Physics of Fluids 35, 036109 (2023)

<https://doi.org/10.1063/5.0139774>



Physics of Fluids

Special Topic:

John Michael Dealy (1937-2024): Celebrating His Life

Guest Editors: Alan Jeffrey Giacomini and Savvas G. Hatzikiriakos

[Submit Today!](#)

Effect of surface radiation on the surface heat flux of two-dimensional hypersonic panel flow

Cite as: Phys. Fluids **35**, 036109 (2023); doi: [10.1063/5.0139774](https://doi.org/10.1063/5.0139774)
Submitted: 23 December 2022 · Accepted: 21 February 2023 ·
Published Online: 13 March 2023

[View Online](#)[Export Citation](#)[CrossMark](#)

Bingfei Yan (严炳蜚), and Guannan Zheng (郑冠男)^{a)}

AFFILIATIONS

Institute of Mechanics, Chinese Academy of Sciences, Beijing, China

^{a)} Author to whom correspondence should be addressed: zhengguannan@imech.ac.cn

ABSTRACT

This article investigates the effect of surface radiation on the surface heat flux of a two-dimensional hypersonic panel flow by comparing the surface heat fluxes of penetrating-radiative-equilibrium cases with those of constant-wall-temperature cases. A Du Fort–Frankel-type difference scheme is applied to cases with different external flow properties and is verified by comparing the results under a constant-wall-temperature boundary condition with self-similar solutions. Both laminar and turbulent flows are considered, and turbulence is modeled using a Baldwin–Lomax turbulence model with the assumption that full-scale turbulence is reached at the leading edge. The results show that the surface heat fluxes for laminar penetrating-radiative-equilibrium cases are greater by the order of 10% than those for constant-wall-temperature cases with the same temperature value at the corresponding points. Though turbulent instances are substantially more difficult, surface heat fluxes of penetrating-radiative-equilibrium cases are fairly similar to those of constant-wall-temperature cases. These results serve as the foundation for a brief discussion of how parameters affect the outcome and the proposal of a modified reference enthalpy method that can be used to predict heat flux when surface radiation causes a streamwise variation in wall temperature.

Published under an exclusive license by AIP Publishing. <https://doi.org/10.1063/5.0139774>

I. INTRODUCTION

Ever since the first launch of the V-2 rocket in the 1940s, hypersonic flow has attracted the attention of researchers. Well-known studies in the field include the National Aerospace Plane (NASP)¹ and the Hyper-X² programs. During the design of a hypersonic aircraft, the problem of high temperatures on its surface has to be handled properly before it is deemed suitable for practical use. In this context, the use of thermal protection systems (TPS) is effective and even essential.

With recent developments in computer technology, computational aerothermoelasticity has attracted more interest and has been applied to a wide range of objects related to hypersonic flows, including TPS, hypersonic inlets, and composite wings.^{3–5} However, even with the availability of high-performance computers, it is not always feasible to implement a full-scale aerothermoelastic analysis using computational fluid dynamics (CFD) and computational thermostructural dynamics (CTSD). Low-fidelity tools might be less accurate than high-fidelity tools, but they impose much less of a burden on computational resources. Culler and McNamara⁶ showed that quasi-static coupling and time-averaged dynamic coupling yielded almost identical results to instantaneous dynamic coupling. For a low-fidelity approximation of the surface heat flux, McNamara and Friedmann⁷ suggested

the use of Eckert's reference enthalpy method.⁸ Xie *et al.*³ analyzed the effect of TPS size on the aerothermoelastic stability of a hypersonic panel by using this method to compute the aerodynamic heat flux. However, Eckert's reference enthalpy neglects the effect of variations in wall temperature on the flow field, which can be relevant for vehicles like the Space Shuttle.^{9,10} A recent study conducted by Yang *et al.*¹¹ reveals that the surface heat flux of radiative-equilibrium cases is significantly different from that of isothermal cases with the same temperature because of the spatial variation in wall temperature. This suggests that when such a kind of variation is present, approximation methods developed for constant-wall-temperature cases, including Eckert's reference enthalpy method, may provide greatly inaccurate predictions on surface heat flux.

In consideration of the application scenarios of the TPS, it is reasonable for the passive TPS to utilize an outer layer that radiates heat to the surrounding and a lower layer that insulates heat.¹² A TPS based on the advanced metallic honeycomb concept, for instance, consists of a thermal insulation layer and a radiation shielding layer.^{6,13} Because of the relatively low thermal conductivity of the outer layers, the temperature at the interface between the layers and the fluid can be greatly different from that at the inner surface of the layers. This also implies a greater streamwise variation in the wall temperature of the flow field.

For more practical purposes, we choose to investigate the effect of surface radiation, or specifically the effect of spatial variation in wall temperature caused by surface radiation, on the surface heat flux of two-dimensional (2D) hypersonic panel flow by looking into penetrating-radiative-equilibrium cases and comparing the results of these cases with those of the corresponding constant-wall-temperature cases. With regard to the practical needs of empirical estimations of surface heat flux, the method to predict surface heat fluxes for laminar cases will also be discussed.

To avoid the influence of chemical reactions, the cases studied in this paper are limited to the Mach number range of 4.5–6.5 and external flow properties corresponding to the Earth’s atmosphere at geometric heights of 25 000–40 000 m.¹⁴ The leading tip of the panel is left out of the discussion, not only because the numerical method applied is less accurate in this area but also because the basic assumptions of boundary-layer flow do not hold so well there.

II. GOVERNING EQUATIONS

An order-of-magnitude analysis of the Navier–Stokes (N–S) equation for steady laminar panel flow reveals that the pressure is nearly constant in the direction normal to the panel. Although this is not necessarily so for hypersonic flow,¹⁰ we will still take the pressure to be constant in the normal direction, since the Mach numbers that we consider are in the lower hypersonic range. To simplify even further, we assume that the velocity of the external flow is constant, and the pressure is then constant in the entire flow field, thus eliminating its streamwise derivative. The derivation of the equations below is omitted for conciseness, but details can be found in numerous relevant articles and textbooks (see, e.g., Refs. 10 and 15).

The governing equations for steady laminar panel flow are as follows:

the continuity equation

$$\frac{\partial(\rho u)}{\partial x} + \frac{\partial(\rho v)}{\partial y} = 0, \tag{1}$$

the momentum equation

$$\rho u \frac{\partial u}{\partial x} + \rho v \frac{\partial u}{\partial y} = \frac{\partial}{\partial y} \left(\mu \frac{\partial u}{\partial y} \right), \tag{2}$$

the energy equation

$$\rho u c_p \frac{\partial T}{\partial x} + \rho v c_p \frac{\partial T}{\partial y} = \frac{\partial}{\partial y} \left(k \frac{\partial T}{\partial y} \right) + \mu \left(\frac{\partial u}{\partial y} \right)^2, \tag{3}$$

and the equation of state

$$p = \rho RT. \tag{4}$$

The viscosity coefficient μ , thermal conductivity k , and specific heat at a constant pressure c_p are assumed to be functions of temperature T . In the calculations, their values are obtained through interpolation based on the available data.^{16,17} The ideal gas law is used for the equation of state because the cases studied in this article do not involve excessively low temperature or high pressure.

The boundary conditions at the outer edge of the flow field are simply

$$y \rightarrow \infty: \quad u \rightarrow u_e, \quad T \rightarrow T_e,$$

where the properties of the external flow outside of the boundary layer are indicated by subscript e .

At the wall boundary, the no-slip condition is imposed,

$$y = 0: \quad u = 0, \quad v = 0.$$

The temperature boundary condition on the wall for a constant-wall-temperature boundary is

$$y = 0; \quad T = T_w.$$

To derive the temperature boundary condition for the penetrating-radiative-equilibrium case, let us first consider the heat convection within the outer layers of the panel. The longitudinal convection of heat within the layers can be neglected, since the vertical scale of the layers should be much smaller than the longitudinal scale, and physically, the vertical gradient should be much greater than the longitudinal gradient. Since we are dealing with steady cases, the penetrating heat flux should be preserved as it passes through the layers. Therefore, the value $k\partial T/\partial y$ should be constant along the vertical direction. Assuming that the heat conductivity for each layer is constant, we may deduce that the temperature is linearly distributed in the vertical direction within each layer. Through simple calculations, we may obtain the penetrating heat flux,

$$q_p = \frac{T|_{y=0} - T_{\text{inner}}}{\sum_i \frac{h_i}{k_i}},$$

where k_i and h_i are the thermal conductivity and thickness of the i th layer, respectively, while T_{inner} is the temperature of the inner surface of the layers. In the calculations, we assume that there are two layers, namely, the radiation shield layer and the thermal insulation layer, and that their properties do not vary with temperature. The properties are set as $k_1 = 0.250$ W/m/K, $h_1 = 2.0$ mm, $k_2 = 0.0258$ W/m/K, and $h_2 = 10.0$ mm, the same as those specified in Ref. 6, and T_{inner} is taken as 300 K. Based on the discussion above, the temperature boundary condition on the wall for a penetrating-radiative-equilibrium boundary is

$$y = 0: \quad k \frac{dT}{dy} = \epsilon \sigma (T^4 - T_{\text{env}}^4) + \frac{T - T_{\text{inner}}}{\sum_i \frac{h_i}{k_i}},$$

where σ is the Stefan–Boltzmann constant, ϵ is the surface emissivity of the wall, and T_{env} is the temperature of the surrounding environment.

In the case of turbulent flow, the order-of-magnitude analysis shows that pressure variation across the boundary layer is still small, and so it can be neglected in boundary-layer approximations.¹⁸ Here, we adopt the zero-equation Baldwin–Lomax model,¹⁹ where the basic form of the governing equations is identical to the laminar case. The physical properties ρ , u , and T are replaced by their time-averaged values, while the coefficients μ and k are modified by the addition of terms μ_T and k_T . For the penetrating-radiative-equilibrium case, we neglect terms that have smaller order of magnitude values than the main terms, and so the boundary conditions are also of the same form as the laminar case.

III. CALCULATION METHOD

The Du Fort–Frankel-type (D–F-type) difference schemes are a type of difference scheme that can be used to solve a variety of equations such as boundary-layer equations, advection–diffusion equations, and even Schrödinger equations.^{4,20,21} In the typical Du Fort–Frankel (D–F) difference method for boundary-layer equations, during the computation process of the diffusive terms, the value of a variable at the current step is replaced by the average of its values at the following streamwise step and the previous streamwise step. This method does not require any iterative calculations, and it is relatively tolerant of the spacing configuration. A D–F-type difference method is adopted in this article because of its outstanding simplicity and stability. The only difference between it and the typical D–F difference method is the application of higher-order expansions to approximate the first-order streamwise derivatives and the assumption that spacings in the y direction are equal (see, e.g., Ref. 15 for the formulation of the typical D–F difference method). Since the calculation method itself is not the focus of this article, the detailed discretization process for laminar cases is relegated to Appendix A.

When turbulence is taken into account, the coefficients μ and k in the momentum equation and the energy equation are replaced by $\mu + \mu_T$ and $k + k_T$, where μ_T and k_T are determined using the Baldwin–Lomax model.¹⁹ The details of the formulation of the coefficients and the underlying reasons are omitted here for conciseness, but we should point out that the laminar-to-turbulent transition is not considered owing to its complexity. Apart from this, the formulation and turbulence-relevant constants utilized are the same as suggested by Baldwin and Lomax.¹⁹

IV. RESULTS AND DISCUSSION

A. Verification of method

Cases subjected to the constant-wall-temperature boundary condition are first investigated in order to assess the method's validity and accuracy. The results are then contrasted with those from self-similar solutions. The surface heat flux deviates notably from the theoretical value at the leading edge, but it quickly returns to the theoretical value as x increases. When the intervals in the x and y directions are $O(10^{-6})$, the maximum relative deviations of the surface heat flux for multiple cases with x coordinate ranging from 0.1 to 2.0 m are found to be of the order of 0.1%.

Owing to a lack of relevant research and experimental data concerning penetrating-radiative-equilibrium boundaries in the literature, the results of cases with such boundaries cannot be verified by comparing with the existing data. For these cases, we validate the convergence of our scheme and our selection of the magnitudes of the intervals in the x and y directions by halving and doubling these intervals in some of the cases and comparing the results with the original ones. Again, the maximum relative deviations of the surface heat flux are of the order of 0.1% for these cases, with the x coordinate ranging from 0.1 to 2.0 m.

So far, we can conclude that the D–F-type difference method used in this article is capable of generating results with sufficient accuracy under certain ranges of flow field properties. Another observation is that the accuracy of the method generally falls slightly when the wall temperature approaches the adiabatic wall temperature. However, for cases with penetrating-radiative-equilibrium boundaries, the wall

temperature should vary greatly from the adiabatic wall temperature except at the leading edge.

B. Overview of results

We now present a brief overview of the results concerning surface heat transfer. Figure 1 shows how the surface temperature varies with the x coordinate for two specific cases subjected to the penetrating-radiative-equilibrium boundary condition: one laminar and one turbulent. While the surface temperature for the turbulent case is higher than that for the laminar case, it falls smoothly with x for both cases.

Although there is a streamwise variation in the wall temperature caused by surface radiation, the streamwise derivative of the temperature is obviously much smaller than its normal derivative, just as suggested by the order-of-magnitude analysis. One might have expected the surface heat transfer to be rather close to that in the constant-wall-temperature cases, but, as suggested by our results, this is not necessarily true.

For brevity, we denote by θ the ratio of the surface heat flux at a specific point under the penetrating-radiative-equilibrium boundary condition to the heat flux at the same point under the constant-wall-temperature boundary condition (with the constant wall temperature taken to be that at the given point in the penetrating-radiative-equilibrium case). The degrees to which θ deviates from 1 indicate the magnitude of the effect of surface radiation on the surface heat flux. They also show the roughly expected amount of relative errors when applying methods based on the results of constant-wall-temperature cases to estimate the surface heat flux in situations where the wall temperature varies spatially because of surface radiation.

For the cases we have investigated, θ varies in the range of 1.00–1.20. The surface heat flux for the penetrating-radiative-equilibrium case is always larger than that for the corresponding constant-wall-temperature case, as shown by the fact that θ is always greater than 1. This is not surprising since for any point on the wall, the upstream wall temperature is always greater than the temperature at

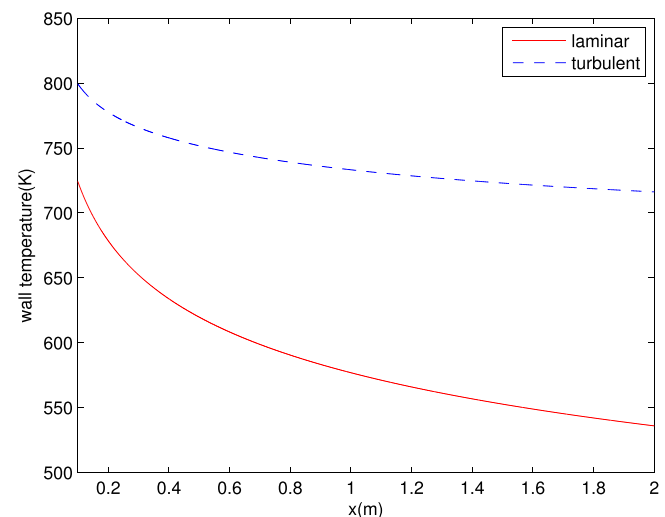


FIG. 1. Variation of wall temperature with x for two sample cases, where $Ma_\infty = 5.0$, height = 30 000 m, and $\varepsilon = 0.7$.

that point, recalling the fact that the wall temperature always decreases with x . In comparison, θ for turbulent cases is much smaller than that for laminar cases, varying only in the range of 1.00–1.06. Additionally, only for small x does θ in turbulent cases vary considerably with x , dropping from values as high as 1.05 at $x = 0.1$ m to as high as 1.03 at $x = 0.4$ m. Since the transition from laminar to turbulent flow is not modeled in our calculation, we expect that the values of θ at larger x would better reflect the circumstance of a full-scale turbulent flow. Assuming that the Baldwin–Lomax model is at least qualitatively correct for our cases and that other effects, such as chemical reactions, are left out, we can deduce that the effect of surface radiation on the surface heat flux for a full-scale turbulent flow is much smaller than that for a laminar flow with the same external flow properties.

Since the focus of this article is on surface heat transfer, the data regarding the Reynolds analogy factor for laminar cases are relegated to Appendix B.

C. Parametric analysis

The main parameters studied in this article are the Mach number, the corresponding geometric height of the external flow, and the surface emissivity. Figures 2–7 show the influence of these parameters on the effect of surface radiation on heat flux. We observe the following:

1. The Mach number is negatively correlated with the ratio θ , for both laminar and turbulent cases. This is mainly because the adiabatic wall temperature and the surface heat flux increase rapidly with the Mach number, thereby diminishing the influence of surface radiation on the surface heat flux from a relative perspective.
2. The corresponding height is negatively correlated with θ for laminar flow. This might result from the increase in external flow temperature with the corresponding height. For turbulent flow, the dependence of θ on the corresponding height is not so apparent, and the reason behind this is yet to be verified.

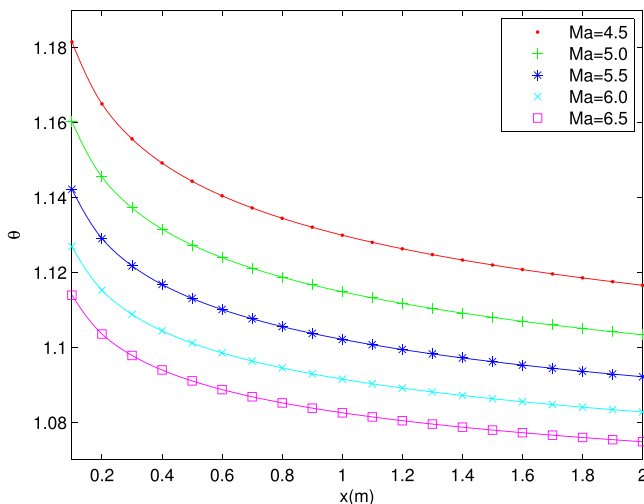


FIG. 2. Variation of θ with x for laminar cases with different Mach numbers, where height = 30 000 m and $\varepsilon = 0.7$.

3. The surface emissivity is negatively correlated with the ratio θ for both laminar and turbulent cases. This may seem counterintuitive in the first place since higher surface emissivity implies a stronger effect of surface radiation. However, a higher surface emissivity brings the wall temperature closer to the temperature of the surrounding environment and the temperature of the inner surface of the panel layers. Intuitively, the x -wall temperature curves of cases with greater values of surface emissivity would be flatter except at the leading edge, and therefore, their surface heat fluxes would be closer to their corresponding constant-wall-temperature cases. In terms of the magnitude of the influence of the parameters on θ , the surface emissivity appears to be less influential than the Mach number and the corresponding height.

D. Implications

It is clear from the results obtained from the D–F-type difference scheme that the ratio θ for laminar flow varies smoothly with x and the parameters, namely, the Mach number, corresponding height, and surface emissivity. The issue is more complicated for turbulent cases, possibly because we have neglected laminar–turbulent transition. However, we have shown that the laminar and turbulent cases exhibit a similar trend in the variation of θ with the Mach number and surface emissivity. This implies that the idea of utilizing a reference enthalpy may still be practicable in situations where surface radiation is present.

The relative error of the calculations in this article conducted using the D–F-type difference method is expected to be $O(0.1\%)$. Modifications to the method, such as reducing the intervals in x and y , are necessary if a higher level of accuracy is required. Apart from this, future studies could focus on the effect of surface radiation on turbulent flows, especially with regard to the stability of laminar boundary layers and the transition from laminar to turbulent flow.

V. MODIFIED REFERENCE ENTHALPY METHOD

Since Eckert’s reference enthalpy method typically provides good predictions on the surface heat fluxes for constant-wall-temperature cases, it should come as no surprise that Eckert’s reference enthalpy method under-predicts the surface heat flux for penetrating-radiative-equilibrium cases by the order of 10%, as shown in Fig. 8.

Based on the results obtained from the D–F-type difference scheme, we propose a modified reference enthalpy method for laminar flow with high surface emissivity. The basic form of this method is assumed to be the same as that of Eckert’s reference method,^{8,10}

$$h^* = \alpha h_e + (1 - \alpha)h_w + \beta r \left(\frac{\gamma - 1}{2} \right) Ma_e^2 h_e, \tag{5}$$

$$C_H^* = \frac{c_1}{(Re_x^*)^{\varepsilon_2}} (Pr^*)^{-2/3}, \tag{6}$$

$$h_{aw} = h_e + r \frac{u_e^2}{2}, \tag{7}$$

$$q_w = \rho^* u_e C_H^* (h_{aw} - h_w). \tag{8}$$

Physical quantities with an asterisk are evaluated at the reference enthalpy,

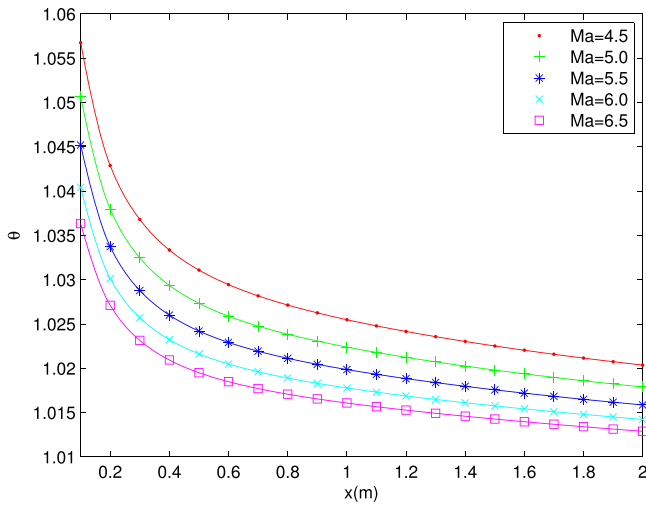


FIG. 3. Variation of θ with x for turbulent cases with different Mach numbers, where height = 30000 m and $\epsilon = 0.7$.

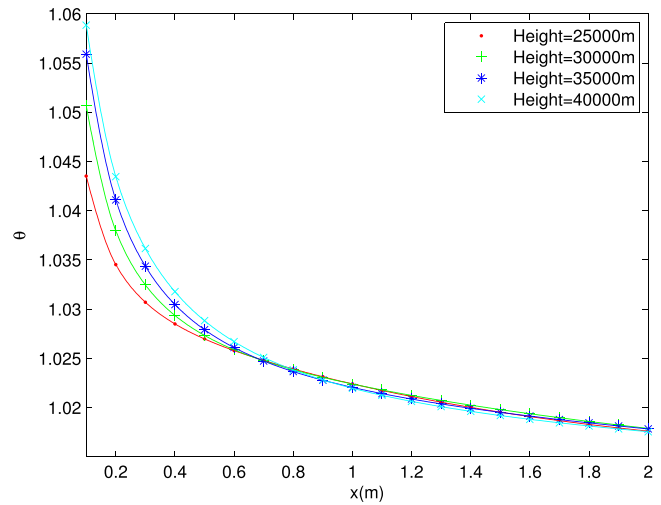


FIG. 5. Variation of θ with x for turbulent cases with different corresponding heights, where $Ma_0 = 5.0$ and $\epsilon = 0.7$.

$$\rho^* = \frac{p_e}{RT^*}, \quad Re_x^* = \frac{\rho^* u_e x}{\mu^*}, \quad Pr^* = \frac{\mu^* c_p^*}{k^*}.$$

Recovery factor r is assumed to be 0.845, and γ is assumed to be 1.4. To determine the value for other parameters, we have chosen α and β as the optimization variables. For each set of values of α and β , the corresponding values of c_1 and c_2 are determined using the weighted nonlinear least squares method and part of the results of penetrating-radiative-equilibrium cases provided by the difference scheme, with the optimization goal being to maximize the coefficient of determination.

The optimal parameters we obtain from the optimization process are $\alpha = 1.12$, $\beta = 0.43$, $c_1 = 0.3688$, and $c_2 = 0.5009$, and the associated coefficient of determination is greater than 0.999. This set of

parameters allows for a good estimation of the surface heat fluxes for penetrating-radiative-equilibrium cases, as shown in Fig. 9. In most cases, the relative difference between surface heat fluxes calculated using this method and those we obtained using the D–F-type difference scheme is less than 2%.

For penetrating-radiative-equilibrium cases, the method can also give a quick and accurate approximation of the wall temperature distribution by setting the estimation of surface heat flux equal to the sum of heat radiated away from the surface and heat penetrating through the surface layers. For instance, if the external flow properties and a specific value of wall temperature are given, the surface heat flux can be obtained from the temperature boundary condition. The expression for the Stanton number and the reference enthalpy can

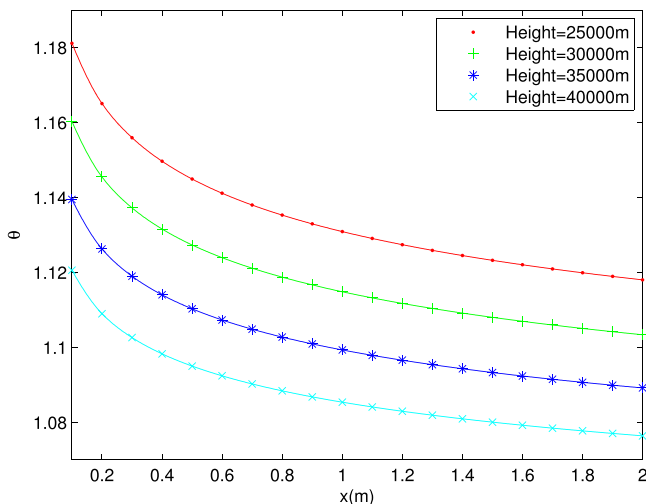


FIG. 4. Variation of θ with x for laminar cases with different corresponding heights, where $Ma_0 = 5.0$ and $\epsilon = 0.7$.

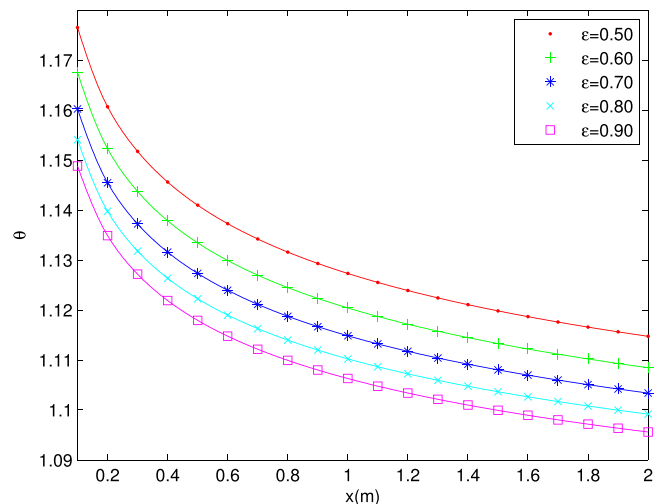


FIG. 6. Variation of θ with x for laminar cases with different surface emissivities, where height = 30000 m and $Ma_0 = 5.0$.

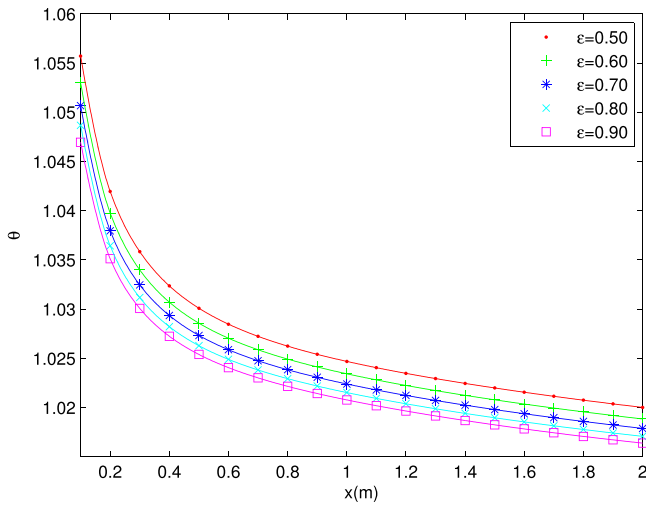


FIG. 7. Variation of θ with x for turbulent cases with different surface emissivities, where height = 30 000 m and $Ma_0 = 5.0$.

then be used to solve the corresponding x . Figure 10 gives an example of how well the surface temperature is estimated using the modified reference enthalpy method for a particular penetrating-radiative-equilibrium case. As can be seen, Eckert's reference enthalpy method under-predicts the surface temperature by around 10–20 K, whereas the approximation of the modified reference enthalpy method deviates no more than 3 K from the results from the difference scheme. Nevertheless, it is important to keep in mind that the accuracy of the modified reference enthalpy method would likely fall if it were applied on the leading edge or on cases where the surface emissivity is too small.

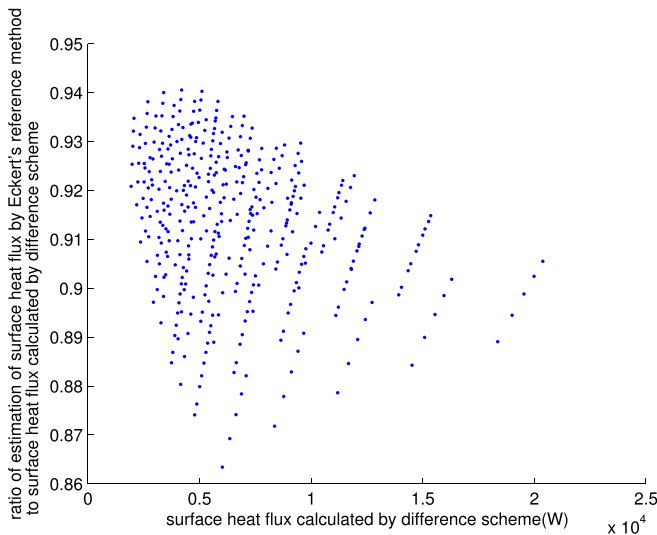


FIG. 8. Scatter diagram of surface heat flux calculated by difference scheme and ratio of estimation of surface heat flux by Eckert's reference enthalpy method to that calculated by difference scheme for penetrating-radiative-equilibrium cases.

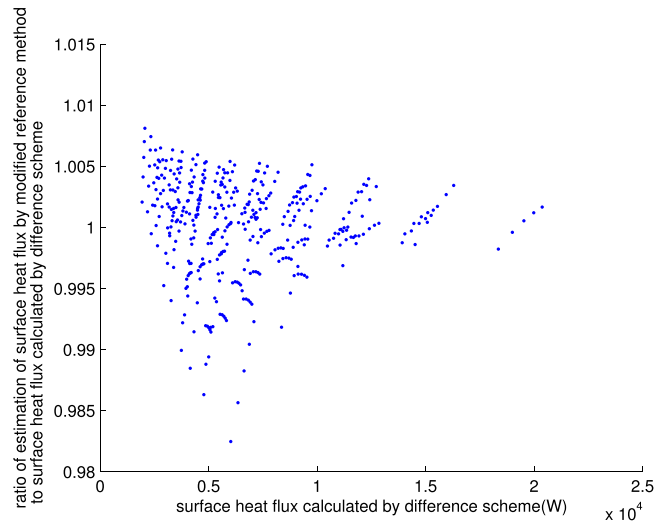


FIG. 9. Scatter diagram of surface heat flux calculated by difference scheme and ratio of estimation of surface heat flux by the modified reference enthalpy method to that calculated by difference scheme for penetrating-radiative-equilibrium cases.

VI. CONCLUSIONS

Laminar and turbulent boundary-layer flows with a penetrating-radiative-equilibrium boundary have both been studied, and it has been discovered that if the spacing is small enough, the Du Fort–Frankel-type difference scheme can provide a sufficient level of accuracy. Although this scheme involves an iterative solution procedure on the wall boundary, it is still relatively easy to implement. Its accuracy has been verified by comparing the results with analytical values as well as the results after halving and doubling the intervals.

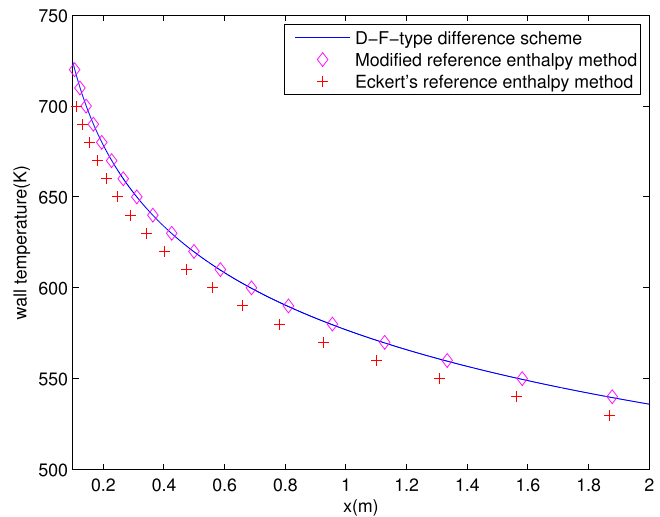


FIG. 10. Comparison of estimated values of wall temperature using reference enthalpy method and numerical results in Sec. IV for a sample laminar case, where height = 30 000 m, $Ma_0 = 5.0$, and $\epsilon = 0.7$.

The heat fluxes for penetrating-radiative-equilibrium cases are, according to the scheme’s results, greater by the order of 10% than those for constant-wall-temperature cases with the same temperature value at the corresponding points. When the Mach number is in the lower hypersonic range or the corresponding height is low, the difference is more pronounced, indicating higher impacts of surface radiation on the surface heat flux. The results have also revealed that Eckert’s reference enthalpy method under-predicts the surface heat flux by the order of 10% when there is a spatial variation in wall temperature brought on by surface radiation.

Based on these results, a modified reference enthalpy method for laminar flow under the influence of surface radiation is proposed, and the parameters are calibrated using an optimization process. The approximations provided by this method match the results from the difference scheme quite well. The findings in this paper have not yet been confirmed by an experiment since there is a dearth of experimental data about penetrating-radiative-equilibrium boundaries in the literature.

The transition from laminar to turbulent flow, streamwise variation in external flow properties, and the difference between steady and unsteady flows are only a few of the significant effects outside the purview of this article that must be taken into account in actual scenarios. Therefore, further research is needed to determine how surface radiation affects the surface heat flux of an actual unsteady boundary-layer flow.

AUTHOR DECLARATIONS

Conflict of Interest

The authors have no conflicts to disclose.

Author Contributions

BingFei Yan: Conceptualization (equal); Methodology (equal); Software (equal); Validation (equal); Visualization (equal); Writing – original draft (equal); Writing – review & editing (equal). **Guannan Zheng:** Resources (equal); Supervision (equal).

DATA AVAILABILITY

The data that support the findings of this study are available from the corresponding author upon reasonable request.

APPENDIX A: DISCRETIZATION PROCESS FOR LAMINAR CASES

The detailed discretization process for laminar cases is as follows:

1. The first-order derivatives in the convective terms of the equations are approximated as

$$\begin{aligned} \left(\frac{\partial \phi}{\partial x}\right)_{ij} &= \frac{2\Delta x_- + \Delta x_{--}}{(\Delta x_+ + \Delta x_-)(\Delta x_+ + \Delta x_- + \Delta x_{--})} \phi_{i+1,j} \\ &\quad - \frac{\Delta x_- - \Delta x_+ + \Delta x_{--}}{\Delta x_{--}(\Delta x_- + \Delta x_+)} \phi_{i-1,j} \\ &\quad - \frac{\Delta x_+ - \Delta x_-}{\Delta x_{--}(\Delta x_+ + \Delta x_- + \Delta x_{--})} \phi_{i-2,j} \\ &\quad + O(\Delta x_{--}^2 + \Delta x_-^2 + \Delta x_+^2) \end{aligned} \tag{A1}$$

and

$$\left(\frac{\partial \phi}{\partial y}\right)_{ij} = \frac{\phi_{i,j+1} - \phi_{i,j-1}}{2\Delta y} + O(\Delta y^2), \tag{A2}$$

where $\Delta x_{--} = x_{i-1} - x_{i-2}$, $\Delta x_- = x_i - x_{i-1}$, and $\Delta x_+ = x_{i+1} - x_i$. In the above expressions, $\phi = u$ for the momentum equation and $\phi = T$ for the energy equation. We have chosen the value of ϕ at step $i - 2$ instead of i in our approximation to enhance the stability of the method.

2. The diffusive terms are approximated as

$$\begin{aligned} \left(\frac{\partial}{\partial y} \left(\lambda \frac{\partial \phi}{\partial y} \right)\right)_{ij} &= \frac{1}{\Delta y} \left(\lambda_{i,j+\frac{1}{2}} \frac{\phi_{i,j+1} - \bar{\phi}_{ij}}{\Delta y} - \lambda_{i,j-\frac{1}{2}} \frac{\bar{\phi}_{ij} - \phi_{i,j-1}}{\Delta y} \right) \\ &\quad + O\left(\frac{\Delta x_-^2 + \Delta x_+^2}{\Delta y^2} + \Delta y^2\right), \end{aligned} \tag{A3}$$

where

$$\begin{aligned} \lambda_{i,j+\frac{1}{2}} &= \frac{1}{2}(\lambda_{ij} + \lambda_{i,j+1}), \\ \lambda_{i,j-\frac{1}{2}} &= \frac{1}{2}(\lambda_{ij} + \lambda_{i,j-1}), \\ \bar{\phi}_{ij} &= \frac{\Delta x_+}{\Delta x_+ + \Delta x_-} \phi_{i-1,j} + \frac{\Delta x_-}{\Delta x_+ + \Delta x_-} \phi_{i+1,j}. \end{aligned}$$

In the above expressions, $\phi = u$ and $\lambda = \mu$ for the momentum equation and $\phi = T$ and $\lambda = k$ for the energy equation. Although a term $O((\Delta x_-^2 + \Delta x_+^2)/\Delta y^2)$ appears in the truncation error, the coefficient of its leading term is $O(\lambda \partial^2 \phi / \partial x^2)$, which is rather small for boundary-layer flow.¹⁵

3. The viscous dissipation term in the energy equation is approximated as

$$\left(\mu \left(\frac{\partial u}{\partial y}\right)^2\right)_{ij} = \mu_{ij} \left(\frac{u_{i,j+1} - u_{i,j-1}}{2\Delta y}\right)^2 + O(\Delta y^2). \tag{A4}$$

4. The continuity equation is approximated as

$$\begin{aligned} \left(\frac{\partial(\rho u)}{\partial x}\right)_{i+1,j+\frac{1}{2}} &= \frac{\Delta x_+}{\Delta x_- (\Delta x_- + \Delta x_+)} \frac{(\rho u)_{i-1,j-1} + (\rho u)_{i-1,j}}{2} \\ &\quad - \frac{\Delta x_- + \Delta x_+}{\Delta x_- \Delta x_+} \frac{(\rho u)_{i,j-1} + (\rho u)_{i,j}}{2} \\ &\quad + \frac{\Delta x_- + 2\Delta x_+}{\Delta x_- (\Delta x_- + \Delta x_+)} \frac{(\rho u)_{i+1,j-1} + (\rho u)_{i+1,j}}{2} \\ &\quad + O(\Delta x_-^2 + \Delta x_+^2) \end{aligned} \tag{A5}$$

and

$$\left(\frac{\partial(\rho v)}{\partial y}\right)_{i+1,j+\frac{1}{2}} = \frac{(\rho v)_{i+1,j+1} - (\rho v)_{i+1,j}}{\Delta y} + O(\Delta y^2). \tag{A6}$$

5. The boundary conditions at the outer edge are specified as

$$u_{i,j_{\max}} = u_e, \quad T_{i,j_{\max}} = T_e.$$

The boundary conditions on the wall are specified as

$$\begin{cases}
 u_{i,1} = 0, \quad v_{i,1} = 0, \\
 T_{i,1} = T_w \quad \text{for a constant-wall-temperature boundary,} \\
 k(T_{i,1}) \frac{4T_{i,2} - T_{i,3} - 3T_{i,1}}{2\Delta y} = \varepsilon\sigma(T_{i,1}^4 - T_e^4) + \frac{T_{i,1} - T_{\text{inner}}}{\sum_p \frac{h_p}{k_p}} \\
 \text{for a penetrating-radiative-equilibrium boundary.}
 \end{cases}$$

In the case of a penetrating-radiative-equilibrium boundary, the wall temperature is solved iteratively.

Since the approximations involve the flow properties from step $i - 2$ to $i + 1$, lower-order approximations are applied at the first and second streamwise steps of the flow field.^{15,22}

APPENDIX B: VARIATION OF THE REYNOLDS ANALOGY FACTOR WITH X

Figures 11–13 show the variation of the Reynolds analogy factor s with x for laminar cases with different parameters. Here, s is given by

$$s = \frac{c_f^*}{2C_H^*}$$

with

$$c_f^* = \frac{\tau_w}{\frac{1}{2}\rho^*u_e^2}, \\
 C_H^* = \frac{q_w}{\rho^*u_e(h_{aw} - h_w)}.$$

The physical quantities with an asterisk are evaluated at the reference enthalpy given by our modified reference enthalpy method, as described in Sec. V

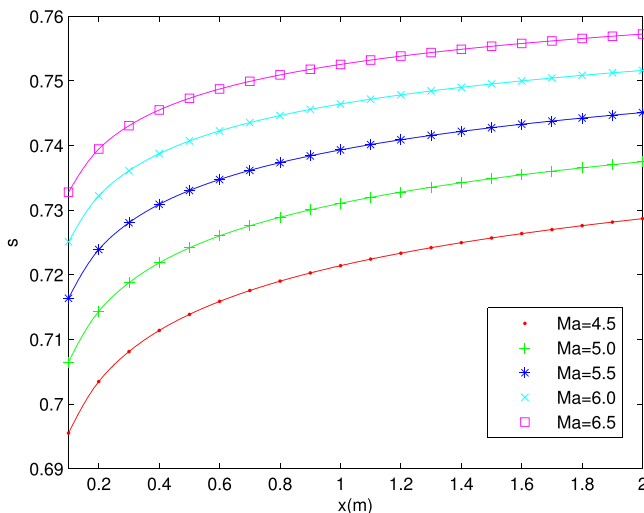


FIG. 11. Variation of Reynolds analogy factor with x for laminar cases with different Mach numbers, where height = 30 000 m and $\varepsilon = 0.7$.

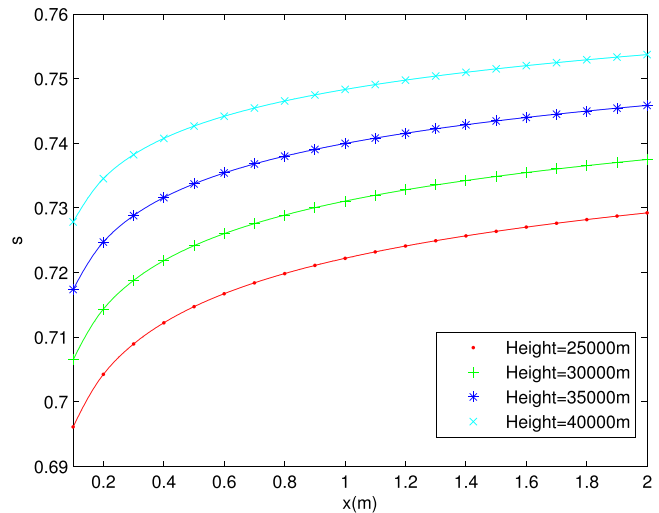


FIG. 12. Variation of Reynolds analogy factor with x for laminar cases with different corresponding heights, where $Ma_e = 5.0$ and $\varepsilon = 0.7$.

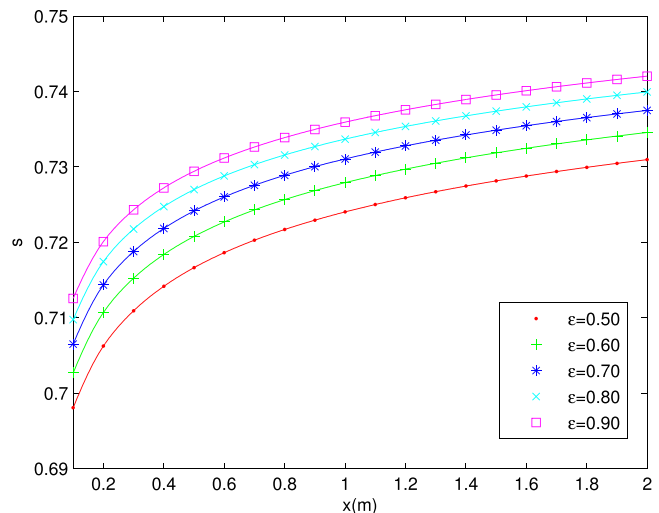


FIG. 13. Variation of Reynolds analogy factor with x for laminar cases with different surface emissivities, where $Ma_e = 5.0$ and height = 30 000 m.

REFERENCES

¹R. Barthélémy, “Recent progress in the National Aerospace Plane program,” *IEEE Aerosp. Electron. Syst. Mag.* **4**(5), 3–12 (1989).
²D. C. Freeman, Jr., D. E. Reubush, C. R. McClinton, V. L. Rausch, and J. L. Crawford, “The NASA Hyper-X program,” U.S. patent NASA/TM-1997-207243 (1 January 1997).
³D. Xie, B. Dong, and X. Jing, “Effect of thermal protection system size on aero-thermoelastic stability of the hypersonic panel,” *Aerosp. Sci. Technol.* **106**, 106170 (2020).
⁴D. Deng and Z. Li, “High-order structure-preserving Du Fort–Frankel schemes and their analyses for the nonlinear schrödinger equation with wave operator,” *J. Comput. Appl. Math.* **417**, 114616 (2023).
⁵K. Ye, Z. Ye, Z. Feng, Y. Pan, and G. Wang, “Numerical investigation on the aerothermoelastic deformation of the hypersonic wing,” *Acta Astronaut.* **160**, 76–89 (2019).

08 April 2024 03:21:07

- ⁶A. J. Culler and J. J. McNamara, "Studies on fluid-thermal-structural coupling for aerothermoelasticity in hypersonic flow," *AIAA J.* **48**, 1721–1738 (2010).
- ⁷J. J. McNamara and P. P. Friedmann, "Aeroelastic and aerothermoelastic analysis in hypersonic flow: Past, present, and future," *AIAA J.* **49**, 1089–1122 (2011).
- ⁸E. R. G. Eckert, "Engineering relations for heat transfer and friction in high-velocity laminar and turbulent boundary-layer flow over surfaces with constant pressure and temperature," *Trans. Am. Soc. Mech. Eng.* **78**, 1273–1283 (1956).
- ⁹D. Kinney, J. Garcia, and L. Huynh, "Predicted convective and radiative aerothermodynamic environments for various reentry vehicles using CBAERO," AIAA Paper No. 2006-659, 2006.
- ¹⁰J. D. Anderson, *Hypersonic and High-Temperature Gas Dynamics*, 2nd ed. (American Institute of Aeronautics and Astronautics, 2006).
- ¹¹Z. Yang, S. Wang, and Z. Gao, "Studies on effects of wall temperature variation on heat transfer in hypersonic laminar boundary layer," *Int. J. Heat Mass Transfer* **190**, 122790 (2022).
- ¹²O. Uyanna and H. Najafi, "Thermal protection systems for space vehicles: A review on technology development, current challenges and future prospects," *Acta Astronaut.* **176**, 341–356 (2020).
- ¹³D. E. Myers, *Parametric Weight Comparison of Advanced Metallic, Ceramic Tile, and Ceramic Blanket Thermal Protection Systems* (National Aeronautics and Space Administration, Langley Research Center, 2000).
- ¹⁴NOAA, NASA, and USAF, *US Standard Atmosphere, 1976* (National Oceanic and Atmospheric Administration, National Aeronautics and Space Administration, and United States Air Force, 1976).
- ¹⁵R. H. Pletcher, J. C. Tannehill, and D. Anderson, *Computational Fluid Mechanics and Heat Transfer* (CRC Press, 2012).
- ¹⁶J. Hilsenrath, *Tables of Thermal Properties of Gases: Comprising Tables of Thermodynamic and Transport Properties of Air, Argon, Carbon Dioxide, Carbon Monoxide, Hydrogen, Nitrogen, Oxygen, and Steam* (US Department of Commerce, National Bureau of Standards, 1955).
- ¹⁷K. Kadoya, N. Matsunaga, and A. Nagashima, "Viscosity and thermal conductivity of dry air in the gaseous phase," *J. Phys. Chem. Ref. Data* **14**, 947–970 (1985).
- ¹⁸T. Cebeci, *Analysis of Turbulent Boundary Layers* (Elsevier, 2012).
- ¹⁹B. Baldwin and H. Lomax, "Thin-layer approximation and algebraic model for separated turbulent flows," AIAA Paper No. 1978-257, 1978.
- ²⁰E. C. D. Fort and S. P. Frankel, "Stability conditions in the numerical treatment of parabolic differential equations," *Math. Tables Other Aids Comput.* **7**, 135–152 (1953).
- ²¹G. Hutomo, J. Kusuma, A. Ribal, A. Mahie, and N. Aris, "Numerical solution of 2-d advection-diffusion equation with variable coefficient using Du-Fort Frankel method," *J. Phys.: Conf. Ser.* **1180**, 012009 (2019).
- ²²R. H. Pletcher, "On a finite-difference solution for the constant-property turbulent boundary layer," *AIAA J.* **7**, 305–311 (1969).